Mechanism of γ-Secretase Cleavage Activation: Is γ-Secretase Regulated through Autoinhibition Involving the Presenilin-1 Exon 9 Loop?

Katharine S. Knappenberger,[§] Gaochao Tian,*[,§] Xiaomei Ye,[#] Cynthia Sobotka-Briner,[§] Smita V. Ghanekar,[‡] Barry D. Greenberg,[⊥] and Clay W. Scott[§]

Departments of Lead Discovery, Medicinal Chemistry, Target Biology, and Neuroscience, AstraZeneca Pharmaceuticals, 1800 Concord Pike, Wilmington, Delaware 19850

Received November 19, 2003; Revised Manuscript Received March 3, 2004

ABSTRACT: Maturation of γ-secretase requires an endoproteolytic cleavage in presenilin-1 (PS1) within a peptide loop encoded by exon 9 of the corresponding gene. Deletion of the loop has been demonstrated to cause familial Alzheimer's disease. A synthetic peptide corresponding to the loop sequence was found to inhibit γ-secretase in a cell-free enzymatic assay with an IC_{50} of 2.1 μM, a value similar to the K_m (3.5 μM) for the substrate C100. Truncation at either end, single amino acid substitutions at certain residues, sequence reversal, or randomization reduced its potency. Similar results were also observed in a cell-based assay using HEK293 cells expressing APP. In contrast to small-molecule γ-secretase inhibitors, kinetic inhibition studies demonstrated competitive inhibition of γ-secretase by the exon 9 peptide. Consistent with this finding, inhibitor cross-competition kinetics indicated noncompetitive binding between the exon 9 peptide and L685458, a transition-state analogue presumably binding at the catalytic site, and ligand competition binding experiments revealed no competition between L685458 and the exon 9 peptide. These data are consistent with the proposed γ-secretase mechanism involving separate substrate-binding and catalytic sites and binding of the exon 9 peptide at the substrate-binding site, but not the catalytic site of γ-secretase. NMR analyses demonstrated the presence of a loop structure with a β-turn in the middle of the exon 9 peptide and a loose α-helical conformation for the rest of the peptide. Such a structure supports the hypothesis that this exon 9 peptide can adopt a distinct conformation, one that is compact enough to occupy the putative substrate-binding site without necessarily interfering with binding of small molecule inhibitors at other sites on γ-secretase. We hypothesize that γ-secretase cleavage activation may be a result of a cleavage-induced conformational change that relieves the inhibitory effect of the intact exon 9 loop occupying the substrate-binding site on the immature enzyme. It is possible that the ΔE9 mutation causes Alzheimer's disease because cleavage activation of γ-secretase is no longer necessary, alleviating constraints on Aβ formation.

Amyloid precursor protein (APP)[1] is a membrane-spanning protein of unknown function, yet its proteolytic processing has pathological significance. One proteolytic fragment of APP, termed Aβ, accumulates as extracellular amyloid deposits in vulnerable brain regions, as one hallmark of Alzheimer's disease. The COOH-terminal 99-amino-acid fragment of APP (C99) is produced by β-secretase cleavage of full-length APP, which is subsequently cleaved by γ-secretase to produce Aβ. The predominant γ-secretase cleavage site occurs following residue 40 of C99, but cleavages also occur following other residues such as 42 or 43, with production of the more fibrilogenic Aβ42 thought to be relatively pathogenic in comparison with Aβ40. The accumulation of the COOH-terminally extended peptides has been associated with increased likelihood for development of Alzheimer's disease (*1*). Certain heritable mutations of the APP gene present on chromosome 21 appear to increase the probability of cleavage occurring at residue 42 (*2*). In addition, FAD mutations in presenilins 1 and 2, homologous transmembrane proteins encoded by genes on chromosomes 14 and 1, respectively, are also associated in cultured cell systems with elevated levels of Aβ42 (*2*).

The disease-association of presenilins is likely linked to their pivotal role in the catalytic activity of γ-secretase, a membrane-associated multicomponent enzyme complex consisting of PS, nicastrin, aph-1, and pen-2 (*3*, *4*). Although the enzyme complex has not been purified or fully character-

* To whom correspondence should be addressed (Tel: 302-886-8137; fax: 302-886-4983; e-mail: gaochao.tian@astrazeneca.com).
[§] Department of Lead Discovery.
[#] Department of Medicinal Chemistry.
[‡] Department of Neuroscience.
[⊥] Department of Target Biology.

[1] Abreviations: Aβ, β amyloid; APP, amyloid protein precursor; CHAPSO, 3-[(3-cholamidopropyl)dimethylammonio]-2-hydoxy-1-propanesulfonate; C99, APP C-terminal fragment of 99 amino acid residues; CNS, central nervous system; COSY, correlated spectroscopy; C100, recombinantly produced C99 containing an additional methionine residue at its N-terminus; DMSO, dimethyl sulfoxide; DMEM, Dulbecco's modification of Eagle's medium; DPBS, Dulbecco's phosphate buffered saline; ECL, electrochemiluminescence; FAD, familial Alzheimer's disease; HI-FBS, heat-inactivated FBS; GαR, goat anti-rabbit; LRP, low-density lipoprotein receptor-related protein; NICD, Notch intracellular domain; NOESY, nuclear Overhauser effect spectroscopy; PC, phosphatidylcholine; PE, phosphatidylethanolamine; PEI, polyethyleneimine; PME, pepstatin A methylester; PS, presenilin; RαAβ40, rabbit anti-Aβ40; RαAβ42, rabbit anti-Aβ42.

10.1021/bi036072v CCC: $27.50
Published on Web 04/27/2004

ized, there is strong evidence that PS may contain the central catalytic unit of the γ-secretase complex (*2*). Two critical aspartate residues are generally required to form the catalytic center of aspartyl proteases, and mutagenesis of two conserved intramembranous aspartate residues (Asp257 and Asp385) of presenilins causes inactivation of γ-secretase (*5*). The intramembranous location of these residues is consistent with a similar location of the scissile bond within the transmembrane domain of the C99 substrate. Furthermore, γ-secretase function is blocked by transition-state isosteres of aspartyl proteases (*6*, *7*), and photochemical derivatives of these inhibitors have been shown to label PS1 (*8*, *9*). These observations have led to the proposal that γ-secretase is an aspartyl protease with PS as its catalytic core (*4*, *5*). However, the possibility remains that presenilins may play a regulatory role, or function as transport or scaffold proteins for the assembly of the catalytic complex (*1*), and that these intramembranous aspartyl mutations may merely disrupt these intermolecular interactions, thereby inactivating the functional complex.

The catalytic mechanism of γ-secretase is unique. Most enzymes bind their substrate and catalyze the reaction by utilizing a single active site. The catalysis by γ-secretase, however, appears to involve two separate centers (*10*−*12*), one specialized for substrate binding and the other for catalysis. To account for the unusual kinetics of this enzyme, we have postulated that a conformational change occurs in the enzyme following binding at the substrate site that moves substrate, or the part containing the scissile bond, into the catalytic center for hydrolysis (*10*, *13*). Adding to its unusual properties is the ability of γ-secretase to process several biologically important transmembrane proteins, including CD44 (*14*, *15*), ErbB4 (*16*), N- and E-cadherin (*17*), LRP (*18*), Nectin-1α (*19*), the Notch ligands Delta and Jagged (*20*), and Notch itself (*21*, *22*). The latter is a key signaling molecule responsible for development of all metazoan species (*23*). Given the importance of these proteins in various biological functions, it is likely that their processing by γ-secretase is tightly controlled. How the substrate specificity of γ-secretase is regulated remains unknown.

PS is a protein of ~50 kDa, predicted to have an eight transmembrane domain topology (*24*, *25*). To form mature, active γ-secretase, the full-length PS is processed endoproteolytically, leading to formation of a stable heterodimeric complex composed of the COOH- and NH_2-terminal PS fragments (*26*−*29*). The endoproteolytic cleavage of PS1 occurs at or near Met298, within a short peptide strand encoded by exon 9 (residues 290−319) (*26*), which is located between transmembrane domains 6 and 7 (*24*, *25*). A FAD-associated PS1 mutant (ΔE9) has been identified in which exon 9 is deleted, due to the mutation of a single nucleotide at the splice acceptor site for exon 9 (*30*). As expected, this deletion prevents the mutant PS1 from undergoing endoproteolysis (*29*). Through mutagenesis analysis, a single point mutation in the exon 9 loop M292D has also been shown to prevent endoproteolysis of PS1 and lead to accumulation of the holoprotein (*31*). Interestingly, rather than producing a catalytically defective γ-secretase, the ΔE9 deletional mutation (*32*) and the M292D point mutation (*31*) result in constitutive activity. The Aβ42 levels and the ratio of Aβ42 over total Aβ are also increased in cells expressing ΔE9 PS1 (*32*). Therefore, it appears that some portion of the exon 9 loop sequence may regulate the γ-secretase activity, the definition of which may help to clarify the unique catalytic mechanism of γ-secretase.

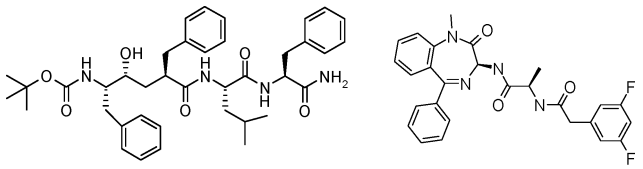

FIGURE 1: Structures of L685458 (a transition-state isostere of γ-secretase) and compound E (a non-transition-state inhibitor).

In this study, we show that a peptide corresponding to the 30-amino-acid sequence encoded by PS1 exon 9 (referred to as "exon 9 peptide") is an inhibitor of γ-secretase in vitro. Smaller peptides were used to examine which amino acids are important in regulating the enzyme activity and to determine the smallest peptide sequence with inhibitory effects. Additional experiments to determine the molecular basis for inhibition were carried out by altering selected amino acids contained in the exon 9 peptide and testing whether binding and inhibition were retained. L685458 and compound E (Figure 1), inhibitors known to bind at different sites on γ-secretase (*13*), were used as tools to elucidate whether the exon 9 peptide binds to the substrate or inhibitor binding sites, or if it binds to a different region in the enzyme complex. COSY and NOESY NMR analyses were performed to elucidate the structural features of the exon 9 peptide and to provide further insights into how the peptide may interact with γ-secretase.

EXPERIMENTAL PROCEDURES

Materials. CHAPSO was purchased from Pierce. Phosphatidylcholine (PC) and phosphatidylethanolamine (PE) were purchased from Avanti Polar-Lipids. Aβ40, Aβ42, RαAβ40, and RαAβ42 were purchased from Biosource. Biotin-4G8 was from SENETEK, Plc. Dynabeads (M-280) were purchased from IGEN. Peptides were obtained from SynPep, Dublin, CA. [^{3}H]L685458, Ru-GαR, C100, and detergent-solubilized human γ-secretase were prepared as described previously (*10*).

Enzyme Reaction and Inhibition Kinetics. Peptides were tested in an enzyme assay to measure inhibition of γ-secretase based on detection of Aβ40 and Aβ42 peptide (*10*). All reactions were run in 96-well microplates containing 25 mM MES, pH 6.5, C100 peptide substrate at a defined concentration, solubilized enzyme (from HeLa cell membrane detergent extract) at 20-fold dilution from stock, inhibitor at defined concentrations diluted from a stock in DMSO (final concentration of DMSO is maintained at 5%), 1 mM EDTA, 1 mM DTT, 0.1 mg/mL BSA, 0.25% CHAPSO, 0.01% PE, and 0.01% PC. The reactions were initiated by addition of enzyme. For IC_{50} determinations, the assay was performed at 37 °C for 3 h prior to addition of detection solution. For kinetic experiments, 40-μL aliquots were quenched at different times by addition of 2 μL of 2 mM PME. To each well (40 μL of reaction mixture), 50 μL of detection solution containing 0.2 μg/mL RαAβ40 or 0.25 μg/mL RαAβ42 and 0.25 μg/mL biotin-4G8 (prepared in DPBS with 0.5%BSA and 0.5% Tween-20) was added and incubated at 4 °C

overnight. Then a 50-μL solution (prepared in the same buffer as above) containing 0.062 μg/mL Ru-GαR and 0.125 mg/mL Dynabeads were added per well. The solutions in 96-well plates were shaken at 25 °C on a plate shaker for 1 h. An additional 60 μL of buffer was added, and the plates were measured for ECL counts in an IGEN M8 analyzer.

Assay of Aβ40 Secretion from HEK293 Cells Transfected with APP. HEK293 cells stably expressing human APP were used this assay. Cells were grown at 37 °C in DMEM containing 10% HI-FBS, 0.5 mg/mL antibiotic−antimycotic solution, and 0.05 mg/mL geneticin, and the cells were harvested when confluent between 80 and 90%. A total of 100 μL cells at a cell density of 1.5 million/mL were added to a flat bottom 96-well cell culture plate (Corning #3595) containing 100 μL of inhibitor in cell culture medium with DMSO at a final concentration of <1%. After the plate was incubated at 37 °C for ~16 h, 100 μL of cell medium was transferred to a round-bottom 96-well plate. To each well of this plate, 50 μL of detection solution containing 0.2 μg/mL RαAβ40 or 0.25 μg/mL RαAβ42 and 0.25 μg/mL biotin-4G8 (prepared in DPBS with 0.5%BSA and 0.5% Tween-20) was added and incubated at 4 °C for 7 h. Then, a 50-μL solution (prepared in the same buffer as above) containing 0.062 μg/mL Ru-GαR and 0.125 mg/mL Dynabeads were added per well. The solutions in 96-well plates were shaken at 22 °C on a plate shaker for 1 h, and the plates were measured for ECL counts in an IGEN M8 analyzer.

Competition Ligand Binding. Radioligand binding assays were performed as described previously (*13*). Briefly, in a 96-well plate, 20 μL of [^{3}H]L685458 (final concentration 1 nM) was mixed with 170 μL of solubilized γ-secretase at a final 10-fold dilution of the stock (prepared at pH 6.5) and 10 μL of unlabeled L685458 or an exon 9-derived peptide (with a final concentration in the range of 100 pM to 30 μM) in DMSO. The mixture was incubated on a plate shaker at room temperature for 30 min, and then filtered through Beckman GF/B 96-well filter-bottom plates (presoaked in 0.6% PEI) using a Packard Filtermate-196, and washed 6 times with 5 mM TrisHCl, pH 7.4. After the filters dried, 30 μL of Microscint20 (Packard) was added to each well, and the plates were counted on a Packard TopCount.

NMR Spectroscopic Analysis of Exon 9 Peptides. Peptide samples were dissolved in H_2O containing 5 or 10% dimethy-d_6 sulfoxide, and 1D proton and 2D COSY and NOESY spectra were acquired on a Bruker AVANCE500 spectrometer equipped with a triple-resonance cryoprobe at either 27 or 10 °C. The strong proton signal of H_2O was suppressed through presaturation in the COSY experiments or by using a water-gated pulse sequence in the NOESY experiments.

Data Analysis. The IC_{50} values were determined by subtracting the background counts (wells without enzyme or cells), determining the percentage of activity (%Act) relative to the maximum wells (those with enzyme and substrate or cells, but no inhibitor), and then fitting the data of %Act as a function of inhibitor concentration according to eq 1:

$$\%\mathrm{Act} = 100\left(1 - \frac{[\mathrm{I}]}{\mathrm{IC}_{50} + [\mathrm{I}]}\right) \tag{1}$$

where I is inhibitor. A standard curve of Aβ40 (or Aβ42) was run in each assay for reference.

Kinetic inhibition data were fit to the following equations, respectively, for competitive, noncompetitive, or uncompetitive inhibition:

$$v = \frac{V_m[\mathrm{S}]}{K_m\left(1 + \frac{[\mathrm{I}]}{K_{is}}\right) + [\mathrm{S}]} \tag{2}$$

$$v = \frac{V_m[\mathrm{S}]}{K_m\left(1 + \frac{[\mathrm{I}]}{K_{is}}\right) + [\mathrm{S}]\left(1 + \frac{[\mathrm{I}]}{K_{ii}}\right)} \tag{3}$$

and

$$v = \frac{V_m[\mathrm{S}]}{K_m + [\mathrm{S}]\left(1 + \frac{[\mathrm{I}]}{K_{ii}}\right)} \tag{4}$$

where V_m and K_m are maximum velocity and the Michaelis−Menten constant, respectively, S is substrate, K_{is} is the inhibitor constant for inhibitor binding to the free enzyme, and K_{ii} is the inhibition constant for inhibitor binding to the ES complex.

For inhibitor cross-competition analyses, inhibition constants were obtained by fitting initial rates to eqs 5 and 6 for noncompetitive and competitive bindings, respectively (*13*):

$$v = \frac{v_0}{\left(1 + \frac{[\mathrm{I}_1]}{K_{i1}} + \frac{[\mathrm{I}_2]}{K_{i2}} + \frac{[\mathrm{I}_1][\mathrm{I}_2]}{\alpha K_{i1} K_{i2}}\right)} \tag{5}$$

and

$$v = \frac{v_0}{\left(1 + \frac{[\mathrm{I}_1]}{K_{i1}} + \frac{[\mathrm{I}_2]}{K_{i2}}\right)} \tag{6}$$

where v_0 is the initial rate in the absence of inhibitor, K_{i1} and K_{i2} are inhibition constants for I_1 and I_2, respectively, and α is the constant defining the interaction between the two inhibitors.

The pattern of cross-competition was analyzed graphically by using the reciprocal of eq 5, which is a linear function of $1/v$ vs $[I_1]$, as given by (*13*):

$$\frac{1}{v} = \frac{1}{v_0}\left(1 + \frac{[\mathrm{I}_2]}{K_{i2}}\right) + \frac{1}{v_0 K_{i1}}\left(1 + \frac{[\mathrm{I}_2]}{\alpha K_{i2}}\right)[\mathrm{I}_1] \tag{7}$$

Changes in $[I_2]$ will have a slope effect if α is close to unity but will have no slope effect if it is infinitely large. Therefore, if the two inhibitors bind simultaneously to the enzyme, the reciprocal plots will intercept to the left of the $1/v$ axis. If binding of one inhibitor excludes the binding of the other, the reciprocal plots will be a set of parallel lines.

Table 1: Summary of IC_{50} Values for Inhibition of γ-Secretase by Exon 9-Derived Peptides[a]

peptide sequence	alteration	IC_{50}, μM Aβ40	IC_{50}, μM Aβ42
STMVWLVNMAEGDPEAQRRVSKNSKYNAES (exon 9)	none	2.1 ± 0.3	3.4 ± 1.8
MVWLVNMAEGDPEAQRRVSKNSKYNAES	N-2	2.3 ± 0.5	
VWLVNMAEGDPEAQRRVSKNSKYNAES	N-3	>200	
WLVNMAEGDPEAQRRVSKNSKYNAES	N-4	>198	
VNMAEGDPEAQRRVSKNSKYNAES	N-6	>190	
EGDPEAQRRVSKNSKYNAES	N-10	>200	
STMVWLVNMAEGDPEAQRRVSKNSKYNA	C-2	31 ± 11	59 ± 15
STMVWLVNMAEGDPEAQRRVSKNSKY	C-4	146 ± 20	
STMVWLVNMAEGDPEAQRRVSKNS	C-6	>159	
STMVWLVNMAEGDPEAQRRV	C-10	>200	
VWLVNMAEGDPEAQRRVSKNSKYNAE	N-3; C-1	>200	>200
MVWLVNMAEGDPEAQRRVSKNSKYNAE	N-2; C-1	2.3 ± 1.1	12 ± 11
IYSSTMVWLVNMAEGDPEAQRRVSKNSKYNAESTER	N+3; C+3	33 ± 7	42 ± 18
IYSSTMVWLVNMAEGDPEAQRRVSKNSKYNAES	N+3	14 ± 2	13 ± 6
STMVWLVNMAEGDPEAQRRVSKNSKYNAESTER	C+3	82 ± 26	48 ± 4
STDVWLVNMAEGDPEAQRRVSKNSKYNAES	M292D	>200	>200
STMVWLVNMAEGDPEAQRRVSKNSKYNAGS	E318G	>200	86 ± 36
STMVWLVNAAEGDPEAQRRVSKNSKYNAES	M298A	142 ± 84	58 ± 22
SEANYKSNKSVRRQAEPDGEAMNVLWVMTS	reverse exon 9	107 ± 20	62 ± 19
ANMMKVDWLARYSSSREQVSNVEKNTGPAE	random exon 9	>200	

[a] Inhibition assays were run in a 50 mM MES buffer, pH 6.5, at 37 °C. Products Aβ40 or Aβ42 were quantitated using the ECL technology and IC_{50} values obtained using eq 1.

Data of ligand competition with [^{3}H]L685458 as the radioligand were analyzed by (*13*):

$$[\mathrm{L685458}]_b = 100\left(1 - \frac{[\mathrm{I}]}{K_i\left(1 + \frac{[\mathrm{L685458}]_t}{K_d}\right) + [\mathrm{I}]}\right) \quad (8)$$

where $[L685458]_b$ is the radioligand bound to γ-secretase, $[L685458]_t$ is the total concentration of L685458 used in assay, K_i is the dissociation constant for I, and K_d is the dissociation constant for L685458.

RESULTS

The Exon 9 Peptide Inhibits γ-Secretase with High Affinity and Sequence Specificity. The exon 9 peptide (STMVWLVNMAEGDPEAQRRVSKNSKYNAES), representing amino acids 290−319 of PS1, was synthesized and tested in an in vitro γ-secretase enzyme assay for Aβ40 production (*10*). This peptide inhibited γ-secretase enzyme activity with an IC_{50} = 2.1 μM (Figure 2A, Table 1), a value comparable to the K_m for the substrate C100 (3.5 μM, see below; 0.6 μM (*10*)). To determine the sequence significance of the peptide, a peptide in the reverse order of exon 9 (reverse exon 9) and another with a randomized sequence were synthesized and tested. The ability to inhibit γ-secretase by these peptides was significantly reduced (by >50-fold) compared to that of the parent peptide (Table 1). Peptides made with single amino acid substitutions corresponding to the FAD-associated point mutation E318G (*33*) (Figure 2A, Table 1) and two cleavage-interfering point mutations M292D and M298A (*31*) also greatly reduced the potency, with mutants E318G and M292D showing no inhibition at concentrations up to 200 μM (Table 1). These data indicate that the exon 9 peptide not only possesses high affinity for γ-secretase but also binds to the enzyme with stringent sequence specificity.

The Optimal Sequence for Inhibition Includes Most of Exon 9. The exon 9 deletion is apparently a random deletion resulting from a point mutation at the splice acceptor site

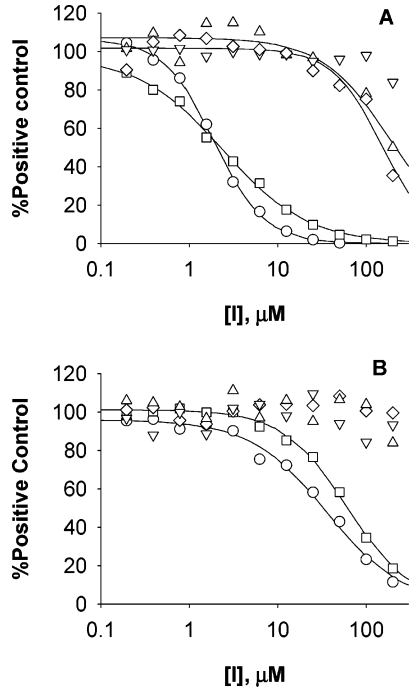

FIGURE 2: Inhibition of Aβ40 production by exon 9 derived peptides. (A) Inhibition of γ-secretase activity in detergent-extracted HeLa cell membranes. The assays were run in a 50 mM MES buffer, pH 6.5, with exon 9 peptide (○), the N-2 and C-1 truncation peptide (□), the N-6 truncation peptide (△), the peptide with E318G point mutation (▽), and the C-6 truncation peptide (◇). The lines are theoretical values calculated using eq 1. (B) Inhibition of Aβ40 secretion from HEK293-APP cells. The assays were performed in DMEM at 37 °C with exon 9 peptide (○), the N-2 and C-1 truncation peptide (□), the N-6 truncation peptide (△), the E318G mutant peptide (▽), and the C-6 truncation peptide (◇). The lines are theoretical values calculated using eq 1.

(*30*). Therefore, it is possible that the peptide encoded by exon 9 is not the optimal length for inhibition of γ-secretase. Truncations and additions to this peptide were generated and tested to define the optimal peptide length for inhibition. Peptides with varying numbers of amino acids deleted from

Table 2: Summary of IC_{50} Values for Inhibition of Aβ-Secretion from HEK293-APP Cells by Exon 9-Derived Peptides[a]

peptide sequence	alteration	IC_{50}, μM
STMVWLVNMAEGDPEAQRRVSKNSKYNAES (exon 9)	none	36 ± 3
MVWLVNMAEGDPEAQRRVSKNSKYNAE	N-2; C-1	60 ± 3
VNMAEGDPEAQRRVSKNSKYNAES	N-6	>200
STMVWLVNMAEGDPEAQRRVSKNS	C-6	>200
STMVWLVNMAEGDPEAQRRVSKNSKYNAGS	E318G	>200

[a] Assays were run by incubating inhibitor with HEK293 cells grown in fresh DMEM containing 10% HI-FBS, 0.1 mg/mL antibiotic/antimycotic, and 0.05 mg/mL genecitin at 37 °C overnight. Newly secreted Aβ40 was quantitated using the ECL technology and IC_{50} values obtained using eq 1.

the NH_2- or COOH-terminus were first tested to determine the minimal sequence required to maintain the inhibitory activity of the exon 9 peptide. Deletion of two amino acid residues at the NH_2-terminus (N-2) did not reduce the potency of the peptide, whereas removal of three or more (N-3, N-4, N-6, and N-10) caused a 100-fold loss of inhibitory activity (Table 1). Deletion of two amino acids at the COOH-terminus (C-2) resulted in a 10-fold reduction in potency, while longer deletions (C-3, C-4, C-6, and C-10) resulted in >70-fold loss of inhibitory activity (Table 1). When two deletions were combined to make a 27-residue peptide (N-2; C-1), an IC_{50} of 2.3 μM (Figure 2A, Table 1) was obtained, a value identical to that measured for the full-length exon 9 peptide (Table 1). Thus, a peptide containing almost the entire exon 9 sequence (90%) is the shortest, "core" sequence that functions as a γ-secretase inhibitor in the Aβ40 assay without a sharp decrease in potency.

Addition of three amino acids to the NH-terminus, the COOH-terminus, or both (using the native PS1 sequence to determine the added residues) also reduced potency for inhibition of γ-secretase (Table 1). When three amino acids were added to the NH_2-terminus (N+3), the IC_{50} increased to 14 μM, while adding three amino acids to the COOH-terminus (C+3) caused a more drastic increase to 83 μM (Table 1). Interestingly, when three amino acids were added to both termini (N+3; C+3), the IC_{50} for the resulting 36-amino-acid peptide was 33 μM (Table 1), a value intermediate to the two individual additions, suggesting that some interplay must exist between these two domains of the peptide inhibitor, insofar as the loss in potency due to these additions is not additive.

Equal Potency for Inhibition of Aβ40 and Aβ42 Production. As shown in Table 1, the exon 9-derived peptides showed a similar rank-order potency for inhibition of Aβ40 and Aβ42 production. This suggests that, even though γ-secretase cleaves APP-derived substrates at multiple sites, the inhibition of these events by exon 9 peptides occurs via the same mechanism, presumably by binding to the same site.

The Exon 9 Peptide and Its Derivatives Inhibit Aβ40 Secretion from HEK293 Cells. To assess if the observed inhibition of γ-secretase in the cell-free, detergent-solubilized cell membranes could be replicated in an intact cellular system, we tested a subset of the exon 9 peptides in a cell-based assay for Aβ40 secretion using HEK293 cells stably expressing APP. This cell-based assay had been routinely used to test small molecule inhibitors of γ-secretase, the result of which correlated well with that of the cell-free enzyme assay (data not shown). As shown in Figure 2B, the exon 9 peptide and the peptide N-2; C-1 inhibited Aβ40 secretion from HEK293-APP cells in a dose−response manner, whereas the peptides with the E318G point mutation and N-6 and C-6 truncations had no effect on Aβ40 secretion at concentrations up to 200 μM. This rank order of potency in the cell-based assay for these peptides (Table 2) was fully in accord with that observed in the enzyme assay although the potency itself was dropped by about an order of magnitude (Figure 2 and Tables 1 and 2). Such a drop of potency from enzyme to cells was not surprising as it had been observed consistently for many small molecule γ-secretase inhibitors (data not shown). The same rank order of potency observed for the exon 9 peptides between the enzyme assay and the cell-based assay, and the fact that none of these peptides showed cytotoxicity (by Alamar Blue assay, data not shown) at all the concentrations used in the cell-based assay, further supported the notion that the observed inhibition of cell-free γ-secretase membrane preparations by the exon 9 peptide was indeed due to the inhibition of the intended target, γ-secretase, and not a result of nonspecific interactions.

The Exon 9 Peptide Inhibits γ-Secretase by Binding Exclusively to the Substrate-Binding Site. The fact that neither a decrease, nor an increase, in the size of the exon 9 peptide is desirable for maintaining the potency of the peptide for inhibition of γ-secretase suggests that the size of the exon 9 loop structure fits a binding pocket on γ-secretase. Previous studies (*10*, *13*) have demonstrated the presence on γ-secretase of at least three binding sites, one for substrate, one for transition-state analogue inhibitors such as L685458 (Figure 1), and another for non-transition-state analogue small molecule inhibitors as represented by compound E (Figure 1). It is unclear on the basis of these data whether the exon 9 peptide binds to one of these, or some other as yet unidentified binding site. To evaluate this, kinetic and radioligand competition assays were performed.

In the kinetic assays, γ-secretase activity was measured while the concentrations of both the substrate and exon 9 peptide were varied. The data obtained in these assays (Figure 3) best fit the competitive model (eq 2) as the double reciprocal plots converge on the $1/v$ axis. This peptide is the first compound to display competitive inhibition of γ-secretase by a rigorous kinetic analysis, as all the small molecule inhibitors studied so far show noncompetitive inhibition (*10*). As tabulated in Table 3, the V_m was 1.1 nM/min, and the K_m for the C100 peptide as determined in this assay was 3.5 μM, while the K_i for the exon 9 peptide equaled 2.7 μM, a value almost identical to the IC_{50} (2.1 μM) (Table 1). Competitive inhibition was also observed for the 27-residue core exon 9 peptide (data not shown). These results suggest that the exon 9 peptide binds to the enzyme at the substrate-binding site.

Table 3: Summary of Inhibition Constants Obtained from Kinetic Inhibition of γ-Secretase, Inhibitor Cross-Competition, and Ligand Competition Binding[a]

experiment	V_m or v_0 pM/min	K_m μM	K_{i1} μM	K_{i2} nM	α
inhibition kinetics					
exon 9	1.1 ± 0.3[b]	3.5 ± 1.5	2.7 ± 0.5		
cross-competition					
exon 9/L685458	0.37 ± 0.02[c]		2.9 ± 0.4	1.7 ± 0.3	1.0 ± 0.4
exon 9/compound E	0.42 ± 0.02[c]		2.8 ± 0.4	0.29 ± 0.04	0.8 ± 0.4
ligand competition					
L685458				5.6 ± 1.5	
N-2 exon 9			>20		

[a] Kinetic inhibition was carried out by varying both the concentration of the exon 9 peptide and that of substrate C100, and the data were analyzed using eq 2 to obtain the kinetic constants. The cross-competition kinetics were performed by the combination of the exon 9 peptide and a noncompetitive inhibitor of $^{\gamma}$-secretase Inhibitor. The data were analyzed using eq 5 to obtain the inhibition constants. The ligand competition binding was conducted with fixed [^{3}H]L685458 (2 nM) and varying amounts of either the exon 9 peptide or the unlabeled L685458. The results were analyzed using eq 8 to extract the inhibition constants. Here, K_{I1} and K_{I2} represent the inhibition constants for the exon 9 peptide and a small molecule inhibitor, respective. [b] V_m. [c] v_0 at [C100] = 0.6 μM.

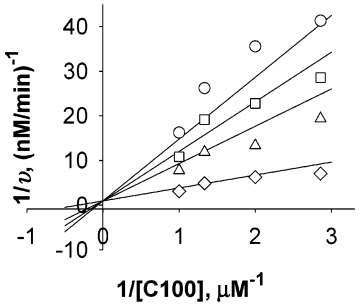

FIGURE 3: Double-reciprocal plots for kinetic inhibition of γ-secretase by the exon 9 peptide. Kinetic assays were run in a 50 mM MES buffer, pH 6.5, with exon 9 peptide at 10 μM (○), 7.5 μM (□), 5 μM (△), and 0 μM (◇). The lines are theoretical values calculated using eq 2. The intercept on the $1/v$ axis in these double-reciprocal plots indicates competitive inhibition.

The exon 9 peptide was also tested in combination with either L685458 or compound E in a series of inhibitor cross-competition analyses. L685458 and compound E were chosen because neither binds to the substrate-binding site (*10*). L685458, a transition-state analogue, likely binds to the catalytic site, whereas compound E apparently binds to a yet undefined site, which is neither the substrate-binding site nor the catalytic site (*10*, *13*). In the inhibitor cross-competition assays, the substrate concentration was held constant while the concentrations of the exon 9 peptide and either L685458 or compound E were changed. The reciprocal plots of the cross-competition data (Figure 4) show an intercepting pattern, indicating that the exon 9 peptide acts noncompetitively with respect to both inhibitors. The K_i value of each compound determined from these experiments (Table 3) is very similar to the values reported previously (*10*). These data are consistent with the exon 9 peptide binding exclusively to the substrate-binding site.

Ligand competition binding experiments using [^{3}H]L685458 as the radioligand were also performed to confirm the kinetic results. As shown in Figure 5, the N-2 exon 9 peptide, which has the same potency as the exon 9 peptide for inhibition of γ-secretase, did not displace [^{3}H]L685458 at concentrations up to 20 μM, a value much greater than its IC_{50} (2.3 μM, Table 1), whereas unlabeled L685458 displaced the radioligand with a K_i of 5.6 nM (Table 3). This confirms that L685458 and the exon 9 peptide do not share a binding site, a result that supports the conclusion that the exon 9 peptide binds exclusively to the substrate-binding site.

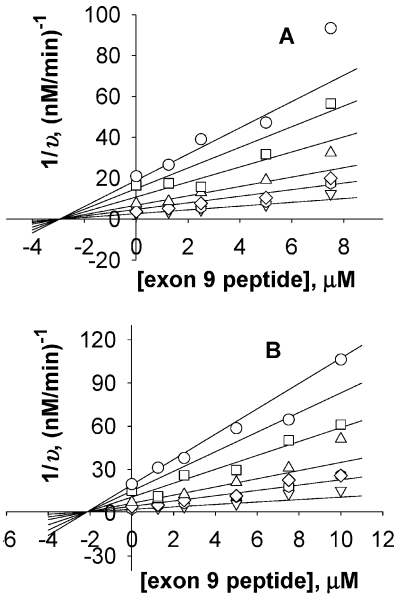

FIGURE 4: Reciprocal plots for inhibitor cross-competition between exon 9 peptide and γ-secretase inhibitors in the γ-secretase assay. (A) Cross-competition between the exon 9 peptide and L685458 tested at [I] = 7.5 nM (○), 5 nM (□), 2.5 nM (△), 1.25 nM (◇), 0.625 nM (⬡), and 0 nM (▽). (B) Cross-competition between the exon 9 peptide and compound E at [I] = 1.5 nM (○), 1 nM (□), 0.5 nM (△), 0.25 nM (◇), 0.125 nM (⬡), and 0 nM (▽). The solid lines are theoretical values calculated using eq 5 with parameters listed in Table 2. The intercepting patterns on these reciprocal plots for inhibitor cross-competition indicate noncompetitive binding of the exon 9 peptide with L6855458 and compound E.

The Exon 9 Peptide Adopts a Dynamic Loop Structure. To gain further insights into the relationship between the activity and structure of the exon 9 peptide, a series of NMR spectroscopic experiments were performed on three peptides that inhibited γ-secretase (exon 9 peptide, N-2; C-1, and N-2), and two inactive peptides, (E318G and N-3).

Analysis of the COSY spectrum (Figure 6A) of the exon 9 peptide in aqueous solution containing 5% DMSO at 27 °C allowed sequential assignments of almost all the residues. A subsequent NOESY analysis of the backbone conformation revealed a NOE between Hα (i) of D13 (counting from the N-terminus of the exon 9 peptide) to Hn (i+3) of A16 that was very weak, but clearly visible at low contour levels (Figure 6B). Also observed were a strong NOE between Hn of E15 and Hn of A16 (Figure 6C) and a very strong NOE

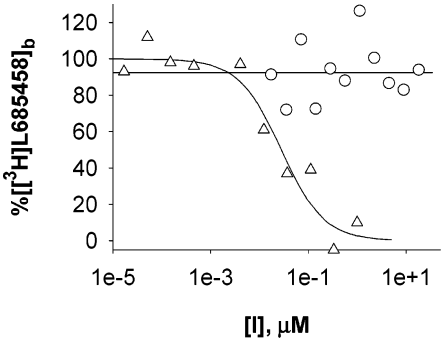

FIGURE 5: Displacement of L685458 by the N-2 exon 9 peptide in the ligand competition binding assay. [^{3}H]L685458 was used as the radioligand and the N-2 exon 9 peptide (○) or the unlabeled L685458 (△) as the competition ligand. The solid curve line for displacement by unlabeled L685458 represents the theoretical values calculated using eq 8, with $K_i = 5.6$, $K_d = 1$ (*13*), and [^{3}H]L685458 = 2 nM. The horizontal line represents the average values of %[^{3}H]L685458]$_b$ obtained in the presence of the N-2 exon 9 peptide at concentrations up to 20 μM.

between Hδ of P14 and Hα of D13 (data not shown). These data demonstrated the presence of a stable β-turn in the middle of the peptide starting at the residue P14. Further NOSEY analysis indicated that most of the peptide adopted a dynamic structure with a loose α-helical conformation, as strong Hα (i) to Hn (i+1) (Figure 6B), medium Hn (i) to Hn (i+1) (Figure 6C), and weak Hα (i) to Hn (i+2) (Figure 6B) NOEs were observed. These observations are consistent with previous predictions of a loop structure for the exon 9 peptide strand in PS1 (*24*, *25*), and support the hypothesis from kinetic inhibition and ligand competition binding studies described above that this exon 9 peptide can adopt a distinct conformation, one that is compact enough to occupy the putative substrate-binding site without necessarily interfering with binding of small molecule inhibitors at other sites on γ-secretase.

The COSY spectra obtained for the two other active peptides and the three inactive peptides were almost identical to that determined for the exon 9 peptide (data not shown), with changes only to the residues directly connected to the mutated residue in E318G. These data indicated that there was no global perturbation of the loop structure by this mutation or reduction in length of the peptide chain, although minor changes in the local structure surrounding the mutated residues could not be ruled out. Therefore, these results suggested that the loss of activity for the E318G point mutation and the N-3 mutation was not due to perturbation of the global structure of the peptide, but rather due to altered interactions of the residues in question with their binding site on the γ-secretase enzyme complex.

DISCUSSION

A general scheme of protease regulation involves the proteolytic activation of a precursor zymogen. Many proteases, such as trypsin (*34*), aspartic proteases (*34*), metalloproteases (*34*), retroviral proteases (*35*), and caspases (*36*), which play a key role in various biologically and pathologically important proteolytic pathways, are initially synthesized as an inactive zymogen, the cleavage of which by an autoproteolytic step or by a second protease is required for activation. In most cases, the two cleavage products usually separate following proteolytic activation, and the inert piece, having no further role in the biology of the active component, is quickly degraded. For most members of caspase family,

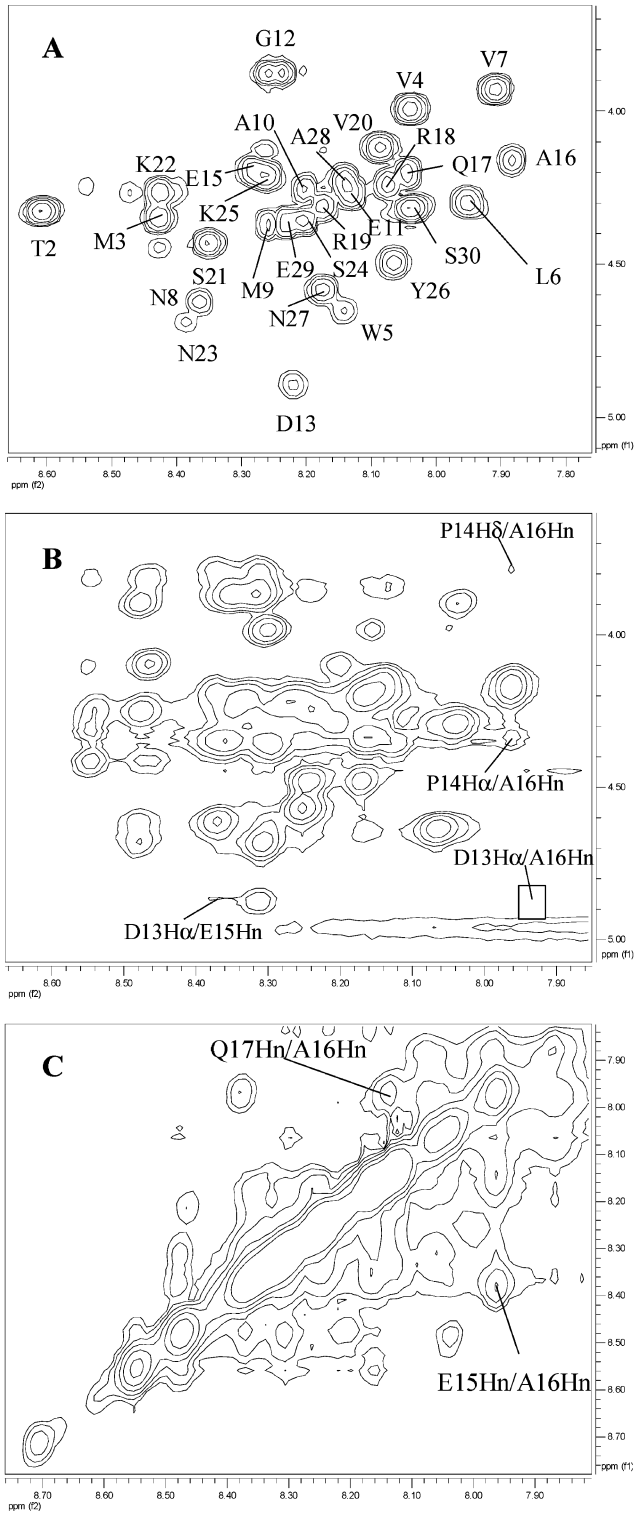

FIGURE 6: NMR spectroscopic analysis of the exon 9 peptide in H_2O with 5% DMSO-d_6. The top panel (A) shows a COSY spectrum of the peptide exon 9 in the region of the cross-peaks between Hα and Hn, obtained at 27 °C with the H_2O signal suppressed by presaturation. Sequential assignment for each residue is labeled as shown in the graph. The middle and bottom panels represent NOESY spectra of the exon 9 peptide in the region of Hα to Hn (B) and Hn to Hn (C), obtained at 10 °C with the H_2O signal suppressed through a watergate pulse program. Several NOEs are shown as labeled. The NOE between D13 Hα and A16 Hn (labeled by the small rectangular in panel B) was very weak and was only observed at the low contour levels.

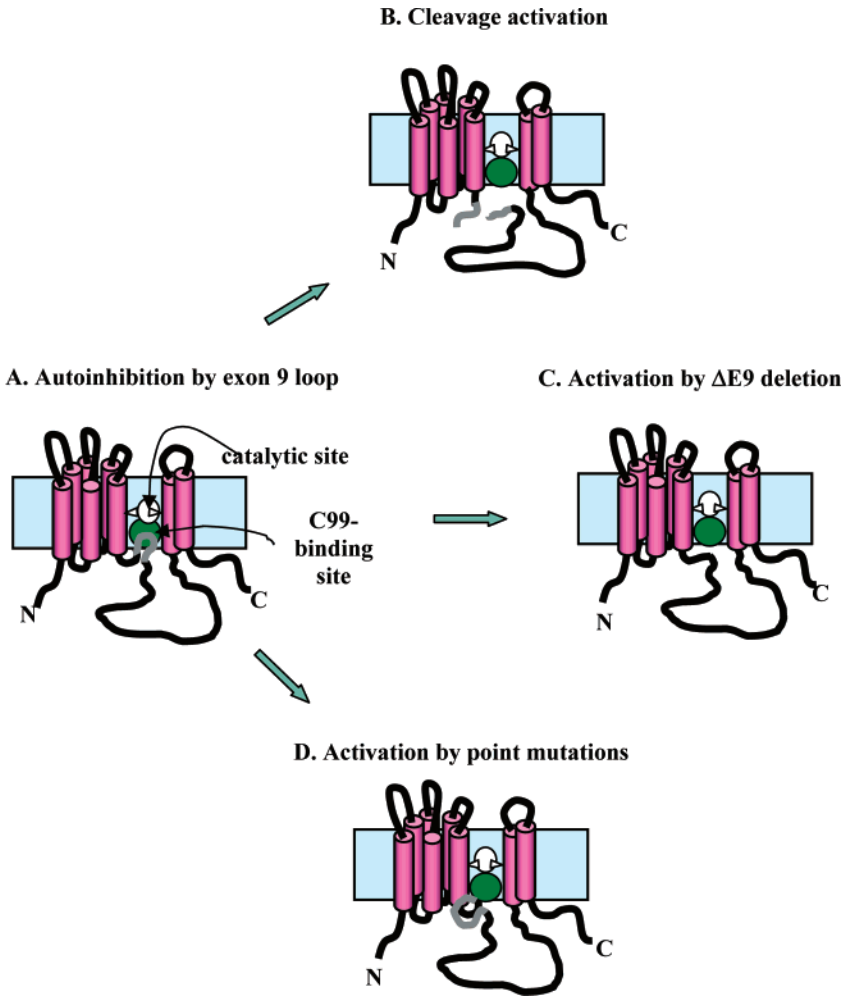

FIGURE 7: Proposed model for cleavage activation of γ-secretase as regulated by the autoinhibitory PS1 exon 9 loop. PS1 transmembrane domains are depicted as cylinders connected by loops (black strands). The exon 9 loop is shown by a short gray strand located within the intracellular loop between transmembrane domains 6 and 7 (counting from left to right). The locations of the putative catalytic aspartate residues are indicated by the arrowheads. The shaded oval represents the substrate-binding site and the white oval represents the putative catalytic site. (A) The intact exon 9 loop (in PS1 holoprotein) sitting in the substrate-binding pocket prevents catalysis. (B) The cleaved exon 9 loop (in the PS1 heterodimer) loses structural integrity and may exit the substrate-binding pocket, thus allowing for substrate to enter and proteolysis to occur. Although broken, the cleaved exon 9 loop may still be able to bind to the substrate pocket, but with less affinity, potentially creating room for modulating enzyme activity by putative regulatory factors. (C) γ-Secretase with PS1 ΔE9 mutation is constitutively active because the exon 9 loop is missing. (D) Structure-perturbing mutations in exon 9 or binding of putative regulatory proteins at or near the exon 9 loop may cause the loop to leave the substrate-binding pocket, resulting in active γ-secretase.

a second cleavage of the monomeric polypeptide results in the formation of a heteromer, with the active site formed at an interface between the two subunits (*36*).

γ-Secretase, which is involved in processing several type-1 transmembrane proteins, is another such example, being activated through an endoproteolytic cleavage within the exon 9 loop of PS, resulting in the formation of a stable complex of NH_2- and COOH-terminal domains (*26*−*29*). Formation of the stable PS1 heterodimeric complex appears necessary for the normal functioning of γ-secretase because two catalytic aspartate residues reside on opposite sides of the scissile bond (*5*). The PS1 ΔE9 mutation, in which the exon 9 loop is deleted and therefore lacks the cleavage activation sites, does not undergo endoproteolysis (*29*). Yet, this mutant is constitutively active (*32*), albeit pathological (*33*). Similarly, the M292D mutation in exon 9 abolishes endoproteolysis but not γ-secretase activity (*31*). Moreover, the observations in this study that the synthetic exon 9 peptide inhibits γ-secretase by binding to the substrate-binding site (Figure 2) with high affinity and sequence specificity (Table 1), supports the logical conclusion that some portion of the loop sequence in the wild-type PS1 plays a role in regulating γ-secretase activity.

The proximity between the exon 9 loop and the putative location of the substrate-binding pocket provides a physical basis for this hypothesis. Assuming that PS1 contains the catalytic center of the enzyme complex (*5*), the catalytic site would be located in the space between the transmembrane domains 6 and 7 (open oval, Figure 7), regions where the two proposed catalytic aspartate residues are located (arrowheads in Figure 7) (*5*). It has been predicted (*12*) that C99 substrate binds to γ-secretase via part of its transmembrane domain that is downstream of the γ-secretase cleavage site, a position located approximately in the middle of the transmembrane domain. Inhibition of γ-secretase by C99-derived peptides supports this conclusion, demonstrating that the COOH-terminal half of the transmembrane domain corresponds to the substrate-binding site on γ-secretase (Sobotka-Briner et al., unpublished data). These predictions place the putative substrate-binding pocket (shaded oval,

Figure 7) adjacent to the catalytic site. According to the proposed topology of PS1 (*24*, *25*), the exon 9 loop (the short gray strand in Figure 7) is linked to the COOH-terminus of the sixth transmembrane domain through a short 26-residue peptide strand (exon 8, residues 264−289). This anchors the exon 9 loop near the edge of the predicted substrate-binding pocket. Such an arrangement affords the exon 9 loop easy access to the putative substrate-binding pocket. Occupation of the substrate pocket by the exon 9 loop would keep the enzyme in a state of autoinhibition (Figure 7A).

Because the exon 9 loop sequence and the core peptide for inhibition of γ-secretase are both neutral and quite lipophilic (*24*, *25*), they are compatible with the hydrophobic environment of the proposed substrate-binding site (*12*). Potential intrastrand salt bridges formed between the four pairs of oppositely charged residues (see amino acid sequence in Table 1) may help to maintain the conformational integrity of the relatively compact, dynamic α-helical exon 9 loop. The 27-residue core exon 9 peptide likely fits into the substrate pocket very well, because minor changes in size by truncation or elongation reduces its potency as a γ-secretase inhibitor (Table 1).

Although a 2.1 μM potency (Table 2) for inhibition of γ-secretase by the exon 9 peptide is only comparable to that of substrate binding (K_m = 3.5 μM, Table 2; 0.6 μM (*10*)), additional thermodynamic affinity for the exon 9 loop is attainable in the full-length PS. In the full-length PS, the exon 9 loop, which is already attached to the enzyme, does not have to overcome the entropy penalty of a free peptide for binding to the substrate-binding pocket. The entropy contribution, together with the intrinsic affinity of the exon 9 loop, could be high enough to eliminate effectively substrate competition for the binding pocket under physiological conditions. When cleaved, however, the exon 9 loop may lose its structural integrity. This conformational deterioration, and the nescient electronic charges at the cleavage site created by the generation of cleavage-mediated NH_2- and COOH-termini, may enable the broken loop to exit the hydrophobic environment of the substrate-binding pocket, freeing the pocket space for substrate binding and cleavage (Figure 7B).

This model of γ-secretase cleavage activation provides a mechanistic basis for the observed biological and pathological function of the PS1 ΔE9 mutation (*32*). The ΔE9 mutant, which lacks the exon 9 loop inhibitory domain, is no longer a zymogen awaiting activation. Rather, it may be constitutively active (Figure 7C). The FAD-associated PS1 ΔE9 deletional mutant also harbors a point mutation S290C and this mutation is responsible for the increased Aβ42 levels observed for cells expressing the ΔE9 mutant PS1 (*32*). To what extent the deletion of exon 9 loop alone may contribute to increased Aβ42 levels remains unclear as the S290C point mutation in the wild-type PS1 has not been evaluated, nor identified in FAD patients. The equal potency (Table 1) observed for the inhibition of γ-secretase-catalyzed Aβ42 and Aβ40 production by the exon 9 peptide suggests that a single substrate-binding site may be involved in the formation of different products such as Aβ42 and Aβ40.

The same model as described above may also explain the functional consequences of the M292D point mutation (*31*), which also results in constitutive γ-secretase activity, as does the deletion of amino acids 292−298 in exon 9 (*31*). Such an abortive endoproteolysis is expected, as amino acid residues 292 and 298 are part of cleavage sites identified in PS1 cleavage activation (*26*). The drastic reduction in inhibitory potency of exon 9 peptides containing M292D (Table 1), or removal of residue 292 (N-3, Table 1), suggests that alteration of the loop structure at residue 292 may weaken the affinity of the exon 9 loop and prevent its binding to the substrate-binding pocket, thereby permitting constitutive activity of the mutant γ-secretase (Figure 7D). The point mutation E318G is the only other known exon 9 mutation that is also FAD-related (*33*). While the precise cause for the disease-association is unclear, the complete loss of inhibitory activity of the corresponding exon 9 peptide (Table 1) suggests that the same mechanism may be operable in the related FAD cases.

It has been proposed that γ-secretase cleavage activation is not a result of autoproteolysis but due to the activity of a yet unidentified "presenilinase" (*37*). While we did not observe any peptide products in the reaction mixture of the exon 9 peptide by mass spectroscopic analysis (data not shown), a result that would be supportive of PS1 processing by a separate enzyme, an attempt to show the product (Aβ40) formation in reaction mixtures containing known γ-secretase substrate (C100) by direct mass spectrometric analysis was unsuccessful (data not shown), probably due to a low turnover (<1%) of substrate during the 3 h reaction time under the same catalytic conditions as used for the exon 9 peptide. This issue awaits further investigation.

An interesting possibility arises from utilizing autoinhibition as a regulatory mechanism, in that naturally occurring regulatory factors might exist that modulate the activity of γ-secretase through interaction with the exon 9 loop. Although the potencies for inhibition of γ-secretase by the exon 9-derived NH_2- or COOH-terminal half peptides are too weak to determine (N-10 and C-10, respectively, Table 1), the cleaved exon 9 loop may retain certain affinity for the substrate-binding pocket. If so, the mature PS1 heterodimeric complex may be subject to regulation through a putative autoinhibitory mechanism that impacts on functions additional to γ-secretase. In this regard, it is worth noting that GSK-3 has been demonstrated to bind PS1 in a region containing the entire exon 8 linker and part of the exon 9 loop (250−298) (*38*). Interestingly, work described in a recent report demonstrates that GSK-3 inhibitors lithium and kenpaullone at concentrations inhibiting GSK-3 activity also block Aβ production both in vitro and in vivo (*39*), although it is not known whether these inhibitors affect the binding interaction of GSK-3 with γ-secretase. A few other proteins are also known to bind PS in this same general region, including α-catenin, β-catenin (binding to residues 330−360) (*40*), tau (binding to residues 250−298) (*38*), and DRAL (binding to residues 269−298) (*41*). The interaction between PS and these proteins appears necessary for PS to exert a modulatory role in the functions of these proteins (*38*, *40*, *41*) or vice versa (*39*). Whether the proposed autoinhibition mechanism involving the exon 9 loop plays a part requires further investigation.

Following synthesis, the full-length PS1 is quickly processed to form a functionally active heterodimeric complex. However, a small fraction of the full-length PS1, although labile with a short half-life (*26*), is detectable in many cells (*26*, *29*, *42*, *43*) and in adult rat (*42*) and human brain (*32*).

While the PS1 holoprotein appears to exist as only a minor fraction, it is intriguing to ponder that a γ-secretase complex containing full-length PS1 may also act as a target for regulation by putative, as yet unidentified regulatory factors.

Several lines of evidence suggest that different substrates may be differentially processed by γ-secretase. For example, certain γ-secretase inhibitors (*44*, *45*) and mutations in presenilins (*43*) appear to affect processing of Notch and APP differently. How the substrate specificity of γ-secretase is regulated remains unknown. γ-Secretase catalysis is unique in that it involves separate sites for substrate binding and catalysis (*10*, *13*). While substrate specificity may be difficult to regulate by only affecting the catalytic site (*13*), perturbing substrate binding or movement of the substrate into the catalytic site could be a more productive way for modulating substrate specificity (*13*), particularly if different substrates bind to different subdomains or subsites on the enzyme complex. The results from the current study indicate that the exon 9 peptide inhibits γ-secretase by binding exclusively to the substrate site, affecting substrate binding without perturbing the catalytic site directly. Further investigation is needed to determine whether regulation of γ-secretase through autoinhibition and cleavage activation plays a role in controlling the substrate specificity of γ-secretase.

ACKNOWLEDGMENT

The authors would like to thank Drs. Frank Liu and John Zysk for preparing C100 and HeLa cell membrane pellets used to prepare detergent extracts of γ-secretase. The authors would also like to thank Mark Sylvester, Ashok Shenvi, and Robert Dedinas for preparation of L685458, [^{3}H]-L685458 and compound E used in this work. Dr. Farzin Gharahdaghi is acknowledged for performing mass spectroscopic analysis of exon 9 peptides. We are grateful for Lois A. Lazor for performing cytotoxicity assays in assessing cytotoxic effects of exon 9 peptides.

REFERENCES

1. Sisodia, S. S., and St. George-Hyslop, P. H. (2002) γ-Secretase, Notch, Aβ and Alzheimer's disease: Where do the presenilins fit in? *Nat. Rev. Neurosci. 3*, 281−290.
2. Wolfe, M. S., and Haass, C. (2001) The role of presenilins in γ-secretase activity. *J. Biol. Chem. 276*, 5413−5416.
3. Edbauer, D., Winkler, E., Regula, J. T., Pesold, B., Steiner, H., and Haass, C. (2003) Reconstitution of γ-secretase activity. *Nat. Cell Biol. 5*, 486−488.
4. De Strooper, B. (2003) Aph-1, pen-2, and nicastrin with presenilin generate an active γ-secretase complex. *Neuron 38*, 9−12.
5. Wolfe, M. S., Xia, W., Ostaszewski, B. L., Diehl, T. S., Kimberly, W. T., and Selkoe, D. J. (1999) Two transmembrane aspartates in presenilin-1 required for presenilin endoproteolysis and γ-secretase activity. *Nature 398*, 513−517.
6. Wolfe, M. S., Xia, W., Moore, C. L., Leatherwood, D. D., Ostazewski, B., Tahmati, T., Donkor, I. O., and Selkoe, D. J. (1999) Peptidomimetic probes and molecular modeling suggest that Alzheimer's γ-secretase is an intramembrane-cleaving aspartyl protease. *Biochemistry 38*, 4720−4727.
7. Shearman, M. S., Beher, D., Clarke, E. E., Lewis, H. D., Harrison, T., Hunt, P., Nadin, A., Smith, A. L., Stevenson, G., and Castro, J. L. (2000) L-685, 458, an aspartyl protease transition state mimic, is a potent inhibitor of amyloid β-protein precursor γ-secretase activity. *Biochemistry 39*, 8698−8704.
8. Li, Y.-M., Xu, M., Lai, M.-T., Huang, Q., Castro, J. L., DiMuzio-Mower, J., Harrison, T., Lellis, C., Nadin, A., Neduvelil, J. G., Register, R. B., Sardana, M. K., Shearman, M. S., Smith, A. L., Shi, X.-P., Yin, K.-C., Shafer, J. A., and Gardell, S. J. (2000) Photoactivated γ-secretase inhibitors directed to the active site covalently label presenilin 1. *Nature 405*, 689−694.
9. Esler, W. P., Kimberly, W. T., Ostaszewski, B. L., Diehl, T. S., Moore, C. L., Tsai, J.-Y., Rahmati, T., Xia, W., Selkoe, D. J., and Wolfe, M. S. (2000) Transition-state analogue inhibitors of γ-secretase bind directly to presenilin-1. *Nat. Cell. Biol. 2*, 428−434.
10. Tian, G., Sobotka-Briner, C. D., Zysk, J., Liu, X., Birr, C., Sylvester, M. A., Edwards, P. D., Scott, C. W., and Greenberg, B. D. (2002) Linear non-competitive inhibition of solubilized human γ-secretase by pepstatin A methylester, L685458, sulfonamides, and benzodiazepines. *J. Biol. Chem. 277*, 31499−31505.
11. Esler, W. P., Kimberly, W. T., Ostaszewski, B. L., Ye, W. J., Diehl, T. S., Selkoe, D. J., and Wolfe, M. S. (2002) Activity-dependent isolation of the presenilin-γ-secretase complex reveals nicastrin and a γ substrate. *Proc. Natl. Acad. Sci. U.S.A. 99*, 2720−2725.
12. Annaert, W. G., Esselens, C., Baert, V., Boeve, C., Snellings, G., Cupers, P., Craessaerts, K., and De Strooper, B. (2001) Interaction with telencephalin and the amyloid precursor protein predicts a ring structure for presenilins. *Neuron 32*, 579−589.
13. Tian, G., Ghanekar, S. V., Aharony, D., Shenvi, A. B., Jacobs, R. T., Liu, X., and Greenberg, B. D. (2003) The Mechanism of γ-Secretase: Multiple inhibitor binding sites for transition state analogs and small molecule inhibitors. *J. Biol. Chem. 278*, 28968−28975.
14. Lammich, S., Okochi, M., Takeda, M., Kaether, C., Capell, A., Zimmer, A.-K., Edbauer, D., Walter, J., Steiner, H., and Haass, C. (2002) Presenilin-dependent intramembrane proteolysis of CD44 leads to the liberation of its intracellular domain and the secretion of an Aβ-like peptide. *J. Biol. Chem. 277*, 44754−44759.
15. Murakami, D., Okamoto, I., Nagano, O., Kawano, Y., Tomita, T., Iwatsubo, T., De Strooper, B., Yumoto, E., and Saya, H. (2003) Presenilin-dependent γ-secretase activity mediates the intramembranous cleavage of CD44. *Oncogene 22*, 1511−1516.
16. Lee, H. J., Jung, K. M., Huang, Y. Z., Bennett, L. B., Lee, J. S., Mei, L., and Kim, T. W. (2002) Presenilin-dependent γ-secretase-like intramembrane cleavage of ErbB4. *J. Biol. Chem. 277*, 6318−6323.
17. Marambaud, P., Shioi, J., Serban, G., Georgakopoulos, A., Sarner, S., Nagy, V., Baki, L., Wen, P., Efthimiopoulos, S., Shao, Z., Wisniewski, T., and Robakis, N. K. (2002) A presenilin-1/γ-secretase cleavage releases the E-cadherin intracellular domain and regulates disassembly of adherens junctions. *EMBO J. 21*, 1948−1956.
18. May, P., Reddy, Y. K., and Herz, J. (2002) Proteolytic processing of low-density lipoprotein Receptor-related protein mediates regulated release of its intracellular domain. *J. Biol. Chem. 277*, 18736−18743.
19. Kim, D. Y., Ingano, L. A. M., Kovacs, D. M. (2002) Nectin-1α, an immunoglobulin-like receptor involved in the formation of synapses, is a substrate for presenilin/γ-secretase-like cleavage. *J. Biol. Chem. 277*, 49976−49981.
20. Ikeuchi, T., and Sisodia, S. S. (2003) The Notch ligands, Delta1 and Jagged2, are substrates for presenilin-dependent "γ-secretase" cleavage. *J. Biol. Chem. 278*, 7751−7754.
21. De Strooper, B., Annaert, W., Cupers, P., Saftig, P., Craessaerts, K., Mumm, J. S., Schroeter, E. H., Schrijvers, V., Wolfe, M. S., Ray, W. J., Goate, A., and Kopan, R. (1999) A presenilin-1-dependent γ-secretase-like protease mediates release of Notch intracellular domain. *Nature 398*, 518−522.
22. Struhl, G., and Greenwald, I. (1999) Presenilin is required for activity and nuclear access of Notch in Drosophila. *Nature 398*, 522−525.
23. Artavanis-Tsakonas, S., Rand, M. D., and Lake, R. J. (1999) Notch signaling: cell fate control and signal integration in development. *Science 284*, 770−776.
24. Doan, A., Thinakaran, G., Borchelt, D. R., Slunt, H. H., Ratovitsky, T., Podlisny, M., Selkoe, D. J., Seeger, M., Gandy, S. E., Price, D. L., and Sisodia, S. S. (1996) Protein topology of presenilin 1. *Neuron 17*, 1023−1030.
25. Li, X., and Greenwald, I. (1998) Additional evidence for an eight-transmembrane-domain topology for *Caenorhabditis elegans* and human presenilins. *Proc. Natl. Acad. Sci. U.S.A. 95*, 7109−7114.
26. Podlisny, M. B., Citron, M., Amarante, P., Sherrington, R., Xia, W., Zhang, J., Diehl, T., Levesque, G., Fraser, P., Haass, C., Koo, E. H. M., Seubert, P., St. George-Hyslop, P., Teplow, D. B., and Selkoe, D. J. (1997) Presenilin proteins undergo heterogeneous endoproteolysis between Thr291and Ala299and occur as stable

N- and C-terminal fragments in normal and Alzheimer brain tissue. *Neurobiol. Dis. 3*, 325−337.
27. Steiner, H., Capell, A., Pesold, B., Citron, M., Kloetzel, P. M., Selkoe, D. J., Romig, H., Mendla, K., and Haass, C. (1998) Expression of Alzheimer's disease-associated presenilin-1 is controlled by proteolytic degradation and complex formation. *J. Biol. Chem. 273*, 32322−32331.
28. Ratovitski, T., Slunt, H. H., Thinakaran, G., Price, D. L., Sisodia, S. S., and Borchelt, D. R. (1997) Endoproteolytic processing and stabilization of wild-type and mutant presenilin. *J. Biol. Chem. 272*, 24536−24541.
29. Thinakaran, G., Borchelt, D. R., Lee, M. K., Slunt, H. H., Spitzer, L., Kim, G., Ratovitsky, T., Davenport, F., Nordstedt, C., Seeger, M., Hardy, J., Levey, A. I., Gandy, S. E., Jenkins, N. A., Copeland, N. J., Price, D. L., and Sisodia, S. S. (1996) Endoproteolysis of presenilin 1 and accumulation of processed derivatives *in vivo*. *Neuron 17*, 181−190.
30. Perez-Tur, J., Froelich, S., Prihar, G., Crook, R., Baker, M., Duff, K., Wragg, M., Busfield, F., Lendon, C., Clark, R. F., Roques, P., Fuldner, R. A., Johnston, J., Cowburn, R., Forsell, C., Axelman, K., Lilius, L., Houlden, H., Karran, E., Roberts, G. W., Rossor, M., Adams, M. D., Hardy, J., Goate, A., Lannfelt, L., and Hutton, M. (1995) A mutation in Alzheimer's disease destroying a splice acceptor site in the presenilin-1 gene. *Neuroreport 7*, 297−301.
31. Steiner, H., Romig, H., Pesold, B., Philipp, U., Baader, M., Citron, M., Loetscher, H., Jacobsen, H., and Haass, C. (1999) Amyloidogenic function of the Alzheimer's disease-associated presenilin 1 in the absence of endoproteolysis. *Biochemistry 38*, 14600−14605.
32. Steiner, H., Romig, H., Grim, M. G., Philipp, U., Pesold, B., Citron, M., Baumeister, R., and Haass, C. (1999) The biological and pathological function of the presenilin-1 Δexon 9 mutation is independent of its defect to undergo proteolytic processing. *J. Biol. Chem. 274*, 7615−7618.
33. Hardy, J. (1997) Amyloid, the presenilins and Alzheimer's disease. *Trends Neurosci. 20*, 154−159.
34. Khan, A. R., and James, M. N. G. (1998) Molecular mechanisms for the conversion of zymogens to active proteolytic enzymes. *Protein Sci. 7*, 815−836.
35. Schatz, G. W., Reinking, J., Zippin, J., Nicholson, L. K., and Vogt, V. M. (2001) Importance of the N-terminus of *Rous sarcoma* virus protease for structure and enzymatic function. *J. Virol. 75*, 4761−4770.
36. Riedl, S. J., Fuentes-Prior, P., Renatus, M., Kairies, N., Krapp, S., Huber, R., Salvesen, G., S., and Bode, W. (2001) Structural basis for the activation of human procaspase-7. *Proc. Natl. Acad. Sci. U.S.A. 98*, 14790−14795.
37. Campbell, W. A., Reed, M. L., Strahle, J., Wolfe, M. S., and Xia, W. (2003) Presenilin endoproteolysis mediated by an aspartyl protease activity pharmacologically distinct from γ-secretase. *J. Neurochem. 85*, 1563−1574.
38. Takashima, A., Murayama, M., Murayama, O., Kohno, T., Honda, T., Yasutake, K., Nihonmatsu, N., Mercken, M., Yamaguchi, H., Sugihara, S., and Wolozin, B. (1998) Presenilin 1 associates with glycogen synthase kinase-3β and its substrate tau. *Proc. Natl. Acad. Sci. U.S.A. 95*, 9637−9641.
39. Phiel, C. J., Wilson, C. A., Lee, V. M.-Y., Klein, P. S. (2003) GSK-3α regulates production of Alzheimer's disease amyloid-β peptides. *Nature 423*, 435−439.
40. Kang, D. E., Soriano, S., Xia, X., Eberhart, C. G., De Strooper, B., Zheng, H., and Koo, E. H. (2002) Presenilin couples the paired phosphorylation of β-catenin independent of axin: implications for β-catenin activation in tumorigenesis. *Cell 110*, 751−762.
41. Tanahashi, H., and Tabira, T. (2000) Alzheimer's disease-associated presenilin 2 interacts with DRAL, an LIM-domain protein. *Hum. Mol. Genet. 9*, 2281−2289.
42. Fraser, P. E., Levesque, G., Yu, G., Mills, L. R., Thirlwell, J., Frantseva, M., Gandy, S. E., Seeger, M., Carlen, P. L., and St George-Hyslop, P. (1998) Presenilin 1 is actively degraded by the 26S proteosome. *Neurobiol. Aging 19*, S19−S21.
43. Capell, A., Steiner, H., Romig, H., Keck, S., Baader, M., Grim, M. G., Baumeister, R., and Haass, C (2000) Presenilin-1 differentially facilitates endoproteolysis of the β-amyloid precursor protein and Notch. *Nat. Cell Biol. 2*, 205−211.
44. Petit, A., Bihel, F., da Costa, C. A., Pourquies, O., Checler, F., and Kraus, J.-L. (2001) New protease inhibitors prevent γ-secretase-mediated production of Aβ40/42 without affecting Notch cleavage. *Nat. Cell Biol. 3*, 507−511.
45. Takahashi, Y., Hayashi, I., Tominari, Y., Rikimaru, K., Morohashi, Y., Kan, T., Natsugari, H., Fukuyama, T., Tomita, T., and Iwatsubo, T. (2003) Sulindac sulfide is a noncompetitive γ-secretase inhibitor that preferentially reduces Aβ42 generation. *J. Biol. Chem. 278*, 18664−18670.

BI036072V